

SUPPORTING INFORMATION ACCOMPANYING:

Dynamic 2D Manganese(II) Isonicotinate Framework with Reversible Crystal-to-Amorphous Transformation and Selective Guest Adsorption

Dariusz Matoga,^{a*} Barbara Gil,^a Wojciech Nitek,^a Alexander D. Todd^b and Christopher W. Bielawski^b

^a*Faculty of Chemistry, Jagiellonian University, Ingardena 3, 30-060 Kraków, Poland. Fax: +48 12 6340515; Tel: +48 12 6632223; E-mail: matoga@chemia.uj.edu.pl*

^b*Department of Chemistry, The University of Texas at Austin, 1 University Station, A1590, Austin, TX 78712, USA*

Contents:

Synthetic procedures	3
Scheme S1. Solvent removal and uptake pathways involving $\{[\text{Mn}_2(\text{ina})_4(\text{H}_2\text{O})_2] \cdot 2\text{EtOH}\}_n$ (1as)	4
SC-XRD data collection and structure refinement details for $\{[\text{Mn}_2(\text{ina})_4(\text{H}_2\text{O})_2] \cdot 2\text{EtOH}\}_n$ (1as)	5
Table S1. Crystal data and structure refinement parameters for $\{[\text{Mn}_2(\text{ina})_4(\text{H}_2\text{O})_2] \cdot 2\text{EtOH}\}_n$ (1as)	5
Table S2. Selected bond lengths (Å) and angles (°) for $\{[\text{Mn}_2(\text{ina})_4(\text{H}_2\text{O})_2] \cdot 2\text{EtOH}\}_n$ (1as)	6
Table S3. Hydrogen bonds for $\{[\text{Mn}_2(\text{ina})_4(\text{H}_2\text{O})_2] \cdot 2\text{EtOH}\}_n$ (1as) (Å and °)	7
Details of other physical measurements	7
Figure S1. PXRD patterns of the as-synthesized $[\text{Mn}(\text{ina})_2]$ (2) compared with $\{[\text{Mn}_2(\text{ina})_4(\text{H}_2\text{O})_2] \cdot 2\text{EtOH}\}_n$ (1as)	8
Figure S2. Asymmetric part of the unit cell of $\{[\text{Mn}_2(\text{ina})_4(\text{H}_2\text{O})_2] \cdot 2\text{EtOH}\}_n$ (1as) with atom labeling scheme and 50% displacement ellipsoids	8
Figure S3. Packing diagrams illustrating interlayer region (parallel to <i>bc</i> plane) of $\{[\text{Mn}_2(\text{ina})_4(\text{H}_2\text{O})_2] \cdot 2\text{EtOH}\}_n$ (1as) filled with removable H_2O and EtOH molecules represented in the spacefill mode. (From top down) Views of three adjacent layers along the [010], [001] and [011] lattice vectors, respectively. Hydrogen atoms are omitted for clarity.	9
Figure S4. UV-vis diffuse reflectance spectra (after Kubelka-Munk transformation) of $\{[\text{Mn}_2(\text{ina})_4(\text{H}_2\text{O})_2] \cdot 2\text{EtOH}\}_n$ (1as), $\{[\text{Mn}_2(\text{ina})_4(\text{H}_2\text{O})_2]\}_n$ (1dea) and $[\text{Mn}(\text{ina})_2]$ (2) (with short description below)	10

Figure S5. IR spectra recorded during activation of $\{[\text{Mn}_2(\text{ina})_4(\text{H}_2\text{O})_2] \cdot 2\text{EtOH}\}_n$ (1as) at increasing temperatures. Bending vibration $\delta(\text{OH})$ at 1228 cm^{-1} , associated with the presence of etoh and responsible for a Franck-Condon progression in the UV-vis diffuse reflectance spectrum.....	11
Figure S6. TG and dTG curves for $\{[\text{Mn}_2(\text{ina})_4(\text{H}_2\text{O})_2] \cdot 2\text{EtOH}\}_n$ (1as) showing stepwise weight loss upon heating (with short description below).	11
Figure S7. <i>In situ</i> IR spectra of $\{[\text{Mn}_2(\text{ina})_4(\text{H}_2\text{O})_2] \cdot 2\text{EtOH}\}_n$ (1as) recorded during n-butanol adsorption at room temperature. (Left) region of OH and CH stretching vibrations; (right) region of skeletal vibrations. (Black line) activated sample; (red line) spectrum recorded after adsorption of excess butanol and its desorption for 5 minutes under vacuum (with short description below).....	12
Figure S8. <i>In situ</i> IR spectra of $\{[\text{Mn}_2(\text{ina})_4(\text{H}_2\text{O})_2] \cdot 2\text{EtOH}\}_n$ (1as) recorded during ethanol adsorption at room temperature. (Left) region of OH and CH stretching vibrations; (right) region of skeletal vibrations. (Black line) activated sample; (red line) spectrum recorded after adsorption of excess ethanol and its desorption for 5 minutes under vacuum (with short description below).....	12
Figure S9. H_2 adsorption isotherm for activated $\{[\text{Mn}_2(\text{ina})_4(\text{H}_2\text{O})_2] \cdot 2\text{EtOH}\}_n$ (1as) at 77K.	13
Estimation of CO_2/N_2 selectivity factor:	13
References in the Supporting Information:	13

Synthetic procedures

All chemicals and solvents (of analytical grade) were purchased from commercial sources (Aldrich, Chempur, POCh, Polmos) and were used as supplied. Ethanol (Polmos) contained water 8% by volume.

Compound $\{[\text{Mn}_2(\text{ina})_4(\text{H}_2\text{O})_2]\cdot 2\text{EtOH}\}_n$ (**1as**)

Isonicotinic acid hydrazide (274 mg, 2.00 mmol) and acetone (700 μL , 10.0 mmol) were dissolved in EtOH (40 mL) and heated under reflux for approx. 15 min. 80% acetic acid (215 μL , 3.00 mmol) was added, and after approx. 5 min. reflux $[\text{Mn}(\text{O}_2\text{CCH}_3)_2]\cdot 4\text{H}_2\text{O}$ (245 mg, 1.00 mmol) was added. Heating under reflux of the resultant yellowish solution was continued for approx. 15 min. The solution was cooled to room temperature, filtered and left for crystallization. After a week dark yellow crystals of **1as** (Yield: 190 mg; 52.3%) were collected, washed with ethanol and dried in air at room temperature. Anal. Calcd for $\text{C}_{28}\text{H}_{32}\text{Mn}_2\text{N}_4\text{O}_{12}$: C, 46.29; H, 4.44; N, 7.71. Found: C, 45.99; H, 4.53; N, 7.70%. Magnetic moment (298 K): $\mu_{\text{ef}} = 5.7 \mu_{\text{B}}$. IR (ATR, cm^{-1}): $\nu(\text{COO})_{\text{as}}$ 1643s 1599vs, $\nu(\text{COO})_{\text{s}}$ 1415s 1396vs, $\nu(\text{CO}_{\text{ethanol}})$ 1049w, 1087w $\nu(\text{CH}_{\text{ethanol}})$ 2972w, $\nu(\text{OH})$ 3271m br. $S_{\text{BET-N}_2} = 4.2 \pm 0.8 \text{ m}^2/\text{g}$ (at 77 K for prior activated sample). UV-vis (solid state) λ , nm: 447, 441, 419, 400, 310sh, 269, 214.

Note:

Filtrations of **1as** were preceded with sonification (approx. 30-60 s) and carried out with the use of G1-G2 filters to remove small quantities of unidentified byproduct from crystals of **1as**

Upscale syntheses:

To verify experimentally the scalability of **1as** synthesis, analogous preparations were repeated for greater quantities of reactants:

a) Isonicotinic acid hydrazide (1.64 g, 12.0 mmol); acetone (3.0 mL); EtOH (150 mL), 80% acetic acid (860 μL , 12.0 mmol); $[\text{Mn}(\text{O}_2\text{CCH}_3)_2]\cdot 4\text{H}_2\text{O}$ (1.47 g, 6.00 mmol). Yield: 1.30 g (59.6%)

b) Isonicotinic acid hydrazide (4.11 g, 30.0 mmol); acetone (7.5 mL); EtOH (250 mL), 80% acetic acid (2.15 mL, 30.0 mmol); $[\text{Mn}(\text{O}_2\text{CCH}_3)_2]\cdot 4\text{H}_2\text{O}$ (3.67 g, 15.0 mmol). Yield: 2.70 g (49.6%)

Compound $\{[\text{Mn}_2(\text{ina})_4(\text{H}_2\text{O})_2]\}_n$ (**1dea**)

Yellow powdered sample **1as** (101.7 mg; 0.2800 mmol) was heated for about 1 hour at 150°C. The sample was weighed immediately after that. Weight loss of 18.3 mg corresponding to the release of two water molecules and two ethanol molecules per formula unit of **1as** was observed. The resulting pale yellow powder of $\{[\text{Mn}_2(\text{ina})_4]\}_n$ (**1**) (83.4 mg; 0.279 mmol) was exposed to air for about 1 hour at ambient temperature. Weight gain of 4.9 mg corresponding to the uptake of two water molecules per formula unit of **1as** was observed. The resulting pale yellow powder of **1dea** (88.3 mg; 0.278 mmol) was obtained. Yield 100%. Anal. Calcd for $\text{C}_{24}\text{H}_{20}\text{Mn}_2\text{N}_4\text{O}_{10}$: C, 45.44; H, 3.18; N, 8.83. Found: C, 45.61; H, 3.10; N, 9.01%. IR (ATR, cm^{-1}): $\nu(\text{COO}_{\text{as}})$ 1609vs, $\nu(\text{COO}_{\text{s}})$ 1405vs 1394vs. UV-vis (solid state) λ , nm: 390sh, 310sh, 272, 210.

Compound $\{[\text{Mn}_2(\text{ina})_4]\cdot 2\text{EtOH}\}_n$ (**1deh**)

Yellow powdered sample **1as** (82.7 mg; 0.228 mmol) was placed in a desiccator over phosphorus pentoxide under reduced pressure ($p \approx 40 \text{ hPa}$) at ambient temperature for about 24 hours. Weight loss of 4.1 mg corresponding to the release of two water molecules per formula unit of **1as** was observed. The resulting yellow powder of **1deh** (78.6 mg, 0.228 mmol) was obtained. Yield: 100%.

SC-XRD data collection and structure refinement details for $\{[\text{Mn}_2(\text{ina})_4(\text{H}_2\text{O})_2]\cdot 2\text{EtOH}\}_n$ (**1as**)

The crystals of **1as** suitable for X-ray analysis were selected from the material prepared as described under Synthetic procedures. Intensity data were collected on Oxford Diffraction SuperNova dual source diffractometer with an Atlas electronic CCD area detector using Mova microfocus Cu-K α radiation source ($\lambda = 1.5418 \text{ \AA}$).

The crystal data, details of data collection and structure refinement parameters are summarized in Table S1. The positions of all non-hydrogen atoms were determined by direct methods using SIR-97.^{S11} All non-hydrogen atoms were refined anisotropically using weighted full-matrix least-squares on F^2 . Refinement and further calculations were carried out using SHELXL-97.^{S12}

All hydrogen atoms bonded with carbon atoms were positioned with an idealized geometry and refined using a riding model with $U_{\text{iso}}(\text{H})$ fixed at $1.2 U_{\text{eq}}$ of C and $1.5 U_{\text{eq}}$ for methyl groups. The hydrogen atoms of both a water molecule and a hydroxyl group were identified on difference Fourier maps and refined using a riding model with $U_{\text{iso}}(\text{H})$ fixed at $1.5 U_{\text{eq}}$ of oxygen atom.

Crystallographic information file (CIF) has been deposited with the Cambridge Crystallographic Data Centre (CCDC): CCDC-938235 (**1as**). Copy of the data can be obtained free of charge via <http://www.ccdc.cam.ac.uk/conts/retrieving.html>, or from the Cambridge Crystallographic Data Centre, 12 Union Road, Cambridge CB2 1EZ, UK; fax: +44 1223 336 033; or e-mail: deposit@ccdc.cam.ac.uk.

Table S1. Crystal data and structure refinement parameters for $\{[\text{Mn}_2(\text{ina})_4(\text{H}_2\text{O})_2]\cdot 2\text{EtOH}\}_n$ (**1as**).

	1as
empirical formula	$\text{C}_{14}\text{H}_{16}\text{MnN}_2\text{O}_6$
formula weight	363.23
crystal size (mm)	0.44x0.25x0.15
crystal system	Monoclinic
space group	$P2_1/c$
a (Å)	10.869(5)
b (Å)	12.130(5)
c (Å)	13.783(4)
α (deg)	90.00
β (deg)	117.75(2)
γ (deg)	90.00
V (Å ³)	1608.2(11)
Z	4
T (K)	293(2)
D_c (Mg/m ³)	1.500
μ (mm ⁻¹)	6.974
reflections measured	22994
reflections unique	3093
reflections observed [$I > 2\sigma(I)$]	2776
R indices [$I > 2\sigma(I)$]	
R	0.0329
wR_2	0.0832
S	0.901

Table S2. Selected bond lengths (Å) and angles (°) for {[Mn₂(ina)₄(H₂O)₂]·2EtOH}_n (**1as**).

Bond lengths	
Mn–X	
Mn1–O18#1	2.1144(18)
Mn1–O19#2	2.1423(15)
Mn1–O28#3	2.1705(15)
Mn1–O30	2.2111(17)
Mn1–N11	2.2584(16)
Mn1–N21	2.2908(18)
C–O (carboxylate)	
O18 –C17	1.227(3)
O19 –C17	1.240(2)
O28 –C27	1.248(2)
O29 –C27	1.248(2)
C–O (ethanol)	
O31 –C32	1.312(4)
closest M···M	
Mn1···Mn1#1	4.909
Bond angles	
O–Mn–O	
O18#1-Mn1-O19#2	99.19(7)
O18#1-Mn1-O28#3	90.11(7)
O19#2-Mn1-O28#3	169.63(6)
O18#1-Mn1-O30	176.93(7)
O19#2-Mn1-O30	83.69(6)
O28#3-Mn1-O30	87.10(7)
O–Mn–N	
O18#1-Mn1-N11	92.39(8)
O19#2-Mn1-N11	88.88(7)
O28#3-Mn1-N11	86.15(6)
O30-Mn1-N11	88.71(7)
O18#1-Mn1-N21	89.11(8)
O19#2-Mn1-N21	89.57(7)
O28#3-Mn1-N21	95.18(7)
O30-Mn1-N21	89.86(7)
N–Mn–N	
N11-Mn1-N21	178.00(6)

Table S3. Hydrogen bonds for $\{[\text{Mn}_2(\text{ina})_4(\text{H}_2\text{O})_2]\cdot 2\text{EtOH}\}_n$ (**1as**) (\AA and $^\circ$).

D-H...A	d(D-H)	d(H...A)	d(D...A)	$\angle(\text{DHA})$
O30-H30A...O29#7	0.76	2.03	2.786(2)	169.0
O30-H30B...O31	0.84	1.84	2.666(3)	171.2
O31-H31...O29#3	0.98	1.75	2.719(3)	167.8

Details of other physical measurements

Carbon, hydrogen and nitrogen were determined using an Elementar Vario MICRO Cube elemental analyzer.

IR spectra were recorded on a Thermo Scientific Nicolet iS5 FT-IR spectrophotometer equipped with an iD5 diamond ATR attachment.

Electronic diffuse reflectance spectra were measured in BaSO_4 pellets with BaSO_4 as a reference using UV-3600 UV-VIS-NIR spectrophotometer equipped with ISR-260 attachment.

Magnetic susceptibility measurements were carried out at room temperature on a Sherwood Scientific Magway MSB MK1 balance.

Gas adsorption studies were performed on a Quantachrome NOVA 2200e surface analyzer. 77K was achieved via an LN_2 bath, and 195K was achieved via dry ice/acetone bath. All measurements pertaining to N_2 were conducted with in-house N_2 . CO_2 and H_2 were supplied by Praxair at 99.998% and 99.995% purity, respectively. All measurements were performed in triplicate and averaged. Specific surface area was determined using a 7-point BET method using molecular nitrogen as the adsorbate. CO_2 (195 K), N_2 (77 K) and H_2 (77 K) isotherm adsorption measurements were performed on degassed samples over a pressure range of 0.01 - 0.90 bar.

Powder X-ray diffraction (PXRD) patterns were recorded at room temperature (295K) on a Rigaku Miniflex 600 diffractometer with $\text{Cu-K}\alpha$ radiation ($\lambda = 1.5418 \text{ \AA}$) in a 2θ range from 3° to 70° with a 0.05° step at a scan speed of 1° min^{-1} .

Thermogravimetric analyses (TGA) were performed on a Mettler-Toledo TGA/SDTA 851^e instrument, coupled with a quadrupole mass spectrometer (QMS) Thermostar GSD 300 T Balzers, at a heating rate of $10^\circ\text{C min}^{-1}$ in a temperature range of 25–600 $^\circ\text{C}$ (sample weight approximately 10 mg). The measurement was performed at atmospheric pressure under flowing argon.

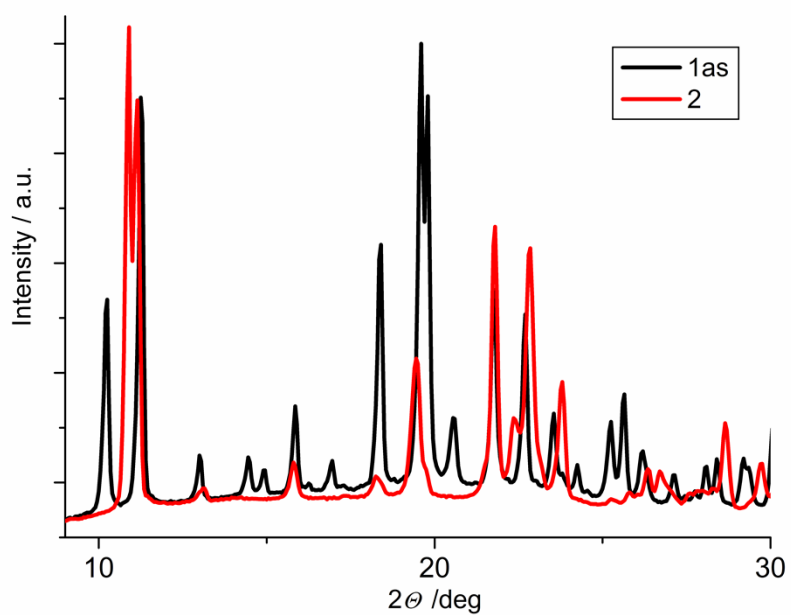


Figure S1. PXRD patterns of the as-synthesized $[\text{Mn}(\text{ina})_2]$ (**2**) compared with $\{[\text{Mn}_2(\text{ina})_4(\text{H}_2\text{O})_2] \cdot 2\text{EtOH}\}_n$ (**1as**).

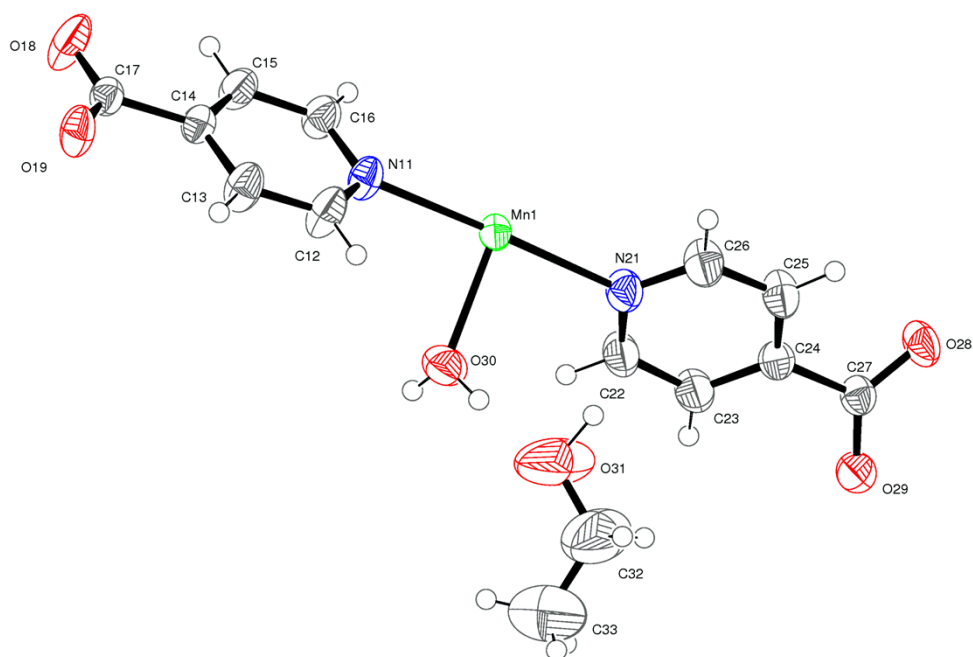


Figure S2. Asymmetric part of the unit cell of $\{[\text{Mn}_2(\text{ina})_4(\text{H}_2\text{O})_2] \cdot 2\text{EtOH}\}_n$ (**1as**) with atom labeling scheme and 50% displacement ellipsoids.

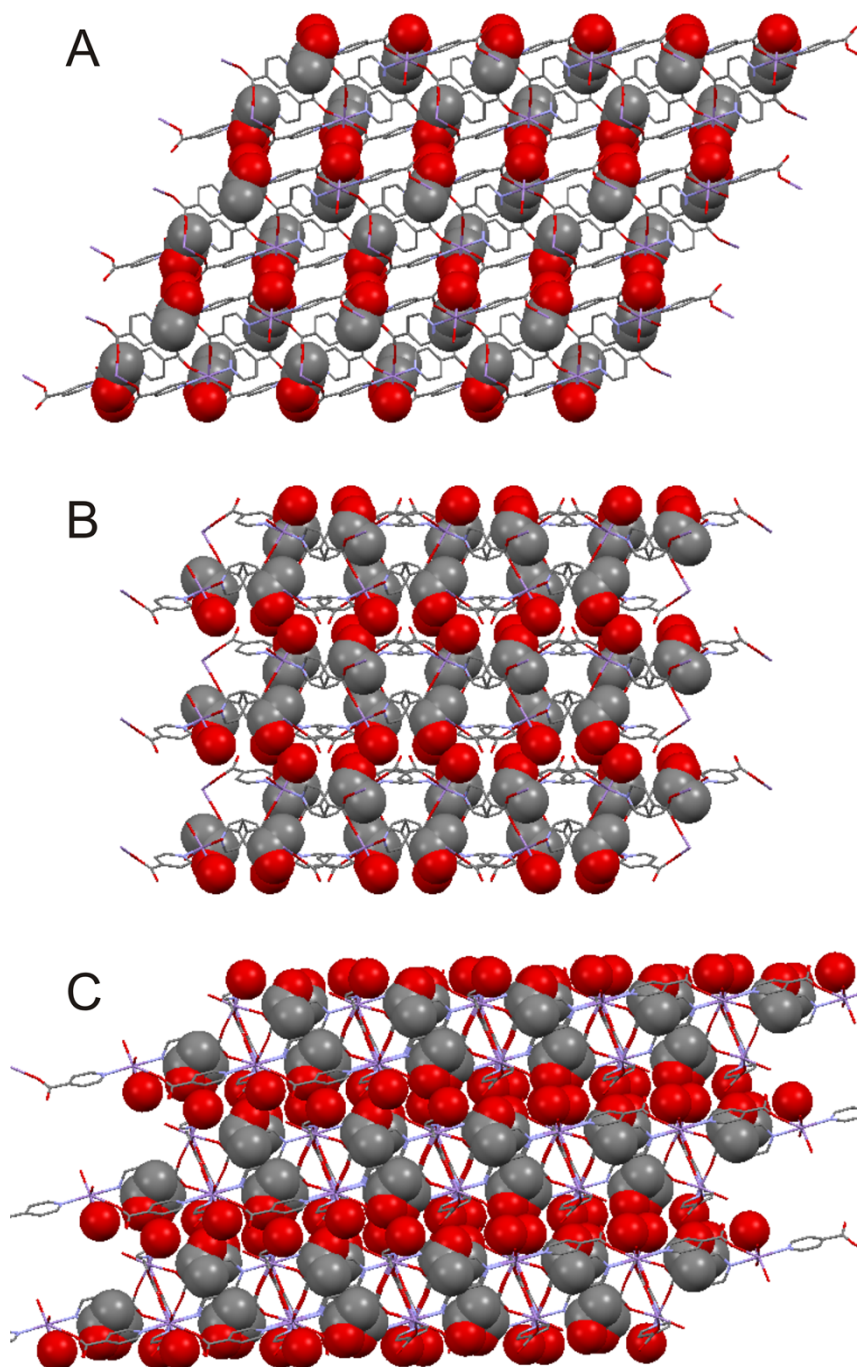


Figure S3. Packing diagrams illustrating interlayer region (parallel to *bc* plane) of $\{[\text{Mn}_2(\text{ina})_4(\text{H}_2\text{O})_2] \cdot 2\text{EtOH}\}_n$ (**1as**) filled with removable H_2O and EtOH molecules represented in the spacefill mode. (From top down) Views of three adjacent layers along the $[010]$, $[001]$ and $[011]$ lattice vectors, respectively. Hydrogen atoms are omitted for clarity.

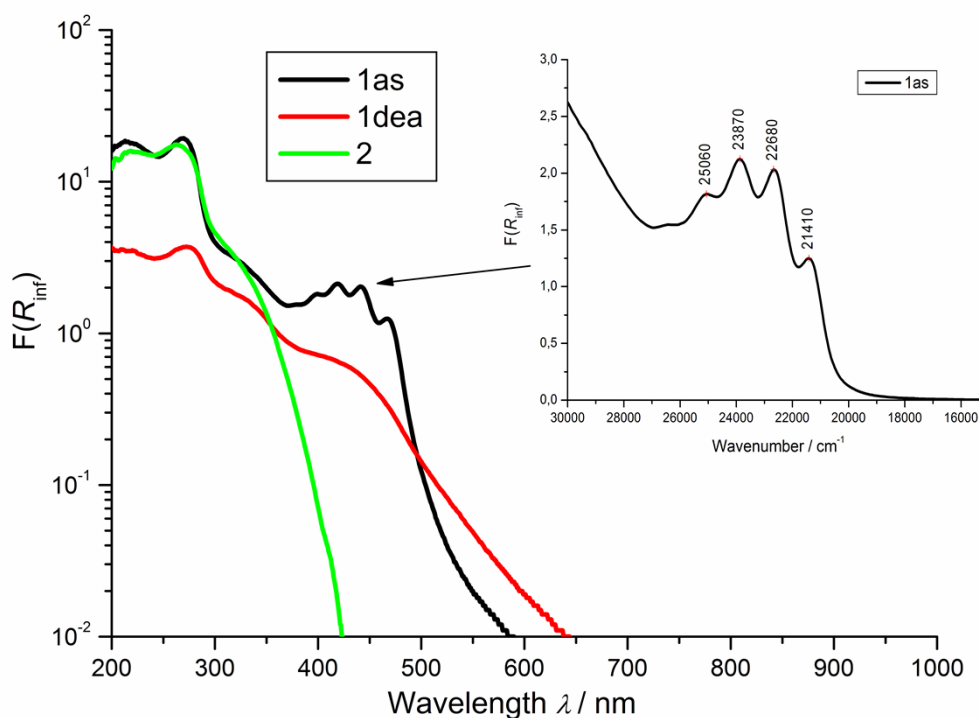


Figure S4. UV-vis diffuse reflectance spectra (after Kubelka-Munk transformation) of $\{[\text{Mn}_2(\text{ina})_4(\text{H}_2\text{O})_2] \cdot 2\text{EtOH}\}_n$ (**1as**), $\{[\text{Mn}_2(\text{ina})_4(\text{H}_2\text{O})_2]\}_n$ (**1dea**) and $[\text{Mn}(\text{ina})_2]$ (**2**) (with short description below).

UV-vis diffuse reflectance spectra for $\{[\text{Mn}_2(\text{ina})_4(\text{H}_2\text{O})_2] \cdot 2\text{EtOH}\}_n$ (**1as**) and $\{[\text{Mn}_2(\text{ina})_4(\text{H}_2\text{O})_2] \cdot 2\text{EtOH}\}_n$ (**1dea**) and $[\text{Mn}(\text{ina})_2]$ (**2**) exhibit three distinct bands in the 200-370 nm range (Fig. S4) at approximately the same positions for all compounds. These are associated with intra-ligand and mlct charge-transfer bands. The spectra of compounds **1as** and **1dea** additionally show lower-energy mlct band at approximately 400 nm which tails into the visible region. Interestingly, this band of **1as** shows a distinct vibrational fine structure with the average $\Delta\nu \sim 1220 \text{ cm}^{-1}$ Franck-Condon progression constant and it disappears upon ethanol removal. In the IR spectrum of **1as** there is a weak band at 1228 cm^{-1} that also disappears upon the alcohol removal (Fig S5). It is ascribed to the $\delta(\text{OH})$ bending vibration of the hydrogen-bonded guest molecules.

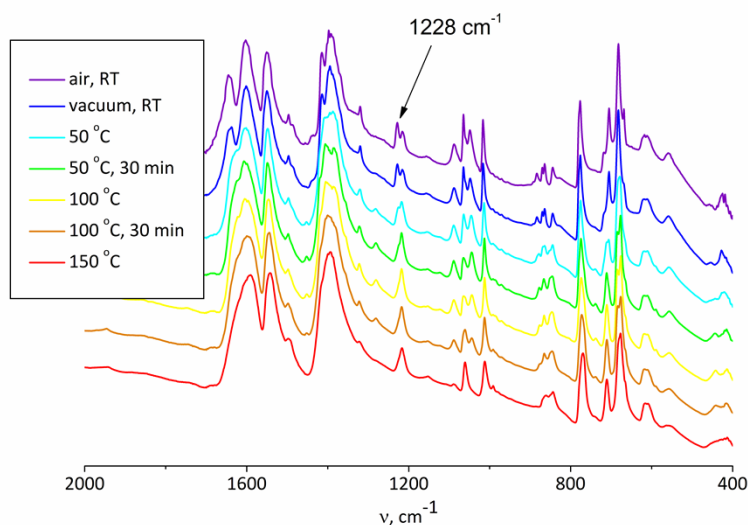


Figure S5. IR spectra recorded during activation of $\{[\text{Mn}_2(\text{ina})_4(\text{H}_2\text{O})_2] \cdot 2\text{EtOH}\}_n$ (**1as**) at increasing temperatures. Bending vibration $\delta(\text{OH})$ at 1228 cm^{-1} , associated with the presence of etoh and responsible for a Franck-Condon progression in the UV-vis diffuse reflectance spectrum.

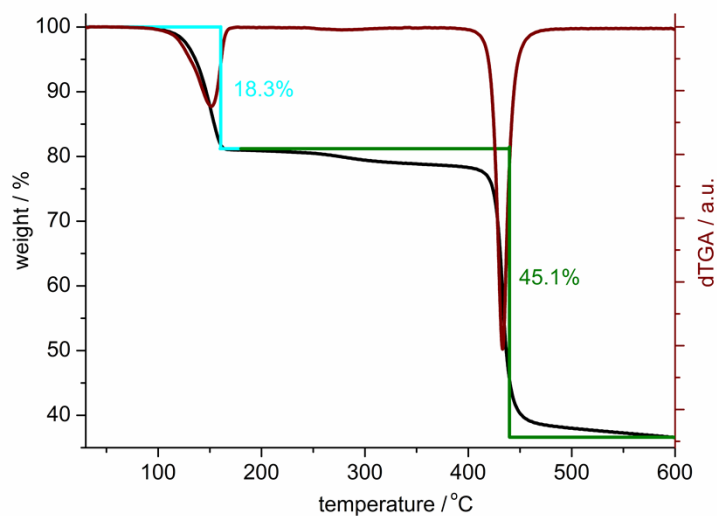


Figure S6. TG and dTG curves for $\{[\text{Mn}_2(\text{ina})_4(\text{H}_2\text{O})_2] \cdot 2\text{EtOH}\}_n$ (**1as**) showing stepwise weight loss upon heating (with short description below).

TGA/QMS for $\{[\text{Mn}_2(\text{ina})_4(\text{H}_2\text{O})_2] \cdot 2\text{EtOH}\}_n$ (**1as**) revealed a stepwise weight loss (Fig. S6) with an approximate plateau in the range 170–400 °C, upon heating. The first distinct step with a maximum at 151 °C corresponds to the loss of two solvate ethanol and two coordination water molecules per formula unit (found: 18.3 %, $m/z = 14$ $[\text{CH}_2]^+$, 15 $[\text{CH}_3]^+$, 17 $[\text{OH}]^+$, 18 $[\text{H}_2\text{O}]^+$; calculated weight-loss: 17.6 %). The final distinct step occurring at 433 °C was assigned to the loss of carboxylate groups (found: 45.1 %, $m/z = 28$ $[\text{CO}]^+$, 44 $[\text{COO}]^+$) and is associated with a decomposition of the compound. Minor discrepancies between found and calculated weight loss in the first step as well as a small weight loss (~3.2%), observed at 280 °C and included in the final step, may be the result of the presence of minor amounts of contaminants in the analysed sample.

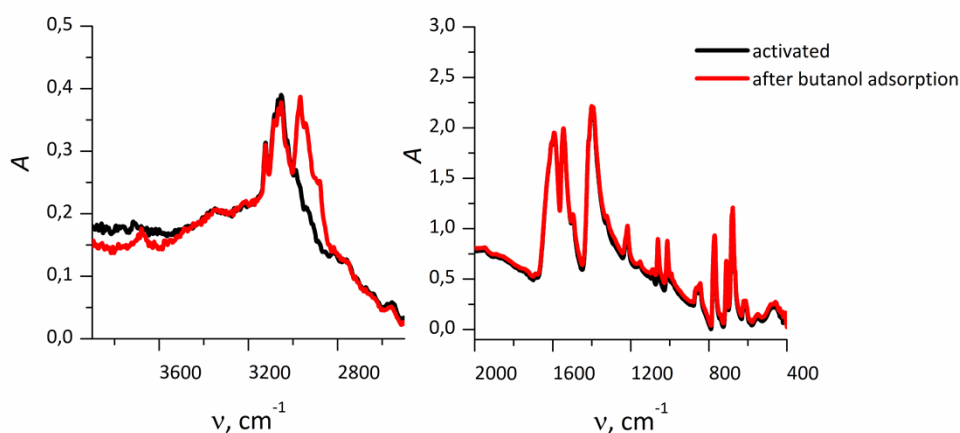


Figure S7. *In situ* IR spectra of $\{[\text{Mn}_2(\text{ina})_4(\text{H}_2\text{O})_2] \cdot 2\text{EtOH}\}_n$ (**1as**) recorded during n-butanol adsorption at room temperature. (Left) region of OH and CH stretching vibrations; (right) region of skeletal vibrations. (Black line) activated sample; (red line) spectrum recorded after adsorption of excess butanol and its desorption for 5 minutes under vacuum (with short description below).

Adsorption of butanol at RT was very weak and even after prolonged contact with sample it was easily desorbed. The most probably it was only adsorbed at the external surfaces of crystallites.

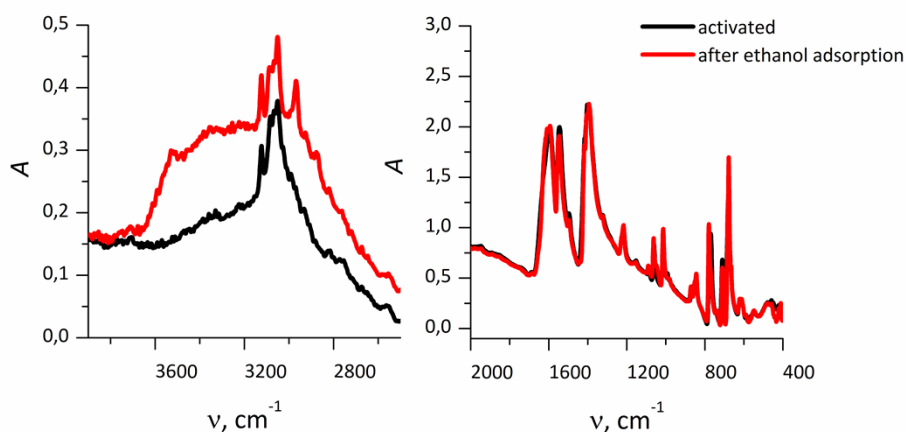


Figure S8. *In situ* IR spectra of $\{[\text{Mn}_2(\text{ina})_4(\text{H}_2\text{O})_2] \cdot 2\text{EtOH}\}_n$ (**1as**) recorded during ethanol adsorption at room temperature. (Left) region of OH and CH stretching vibrations; (right) region of skeletal vibrations. (Black line) activated sample; (red line) spectrum recorded after adsorption of excess ethanol and its desorption for 5 minutes under vacuum (with short description below).

Adsorption of ethanol was performed from the gas phase and the presence of hydrogen-bonded ethanol even after its evacuation confirms its sorption in between MOF layers. In the region of skeletal vibrations there are only small changes, and the spectrum of MOF after ethanol sorption is resembling the one before activation.

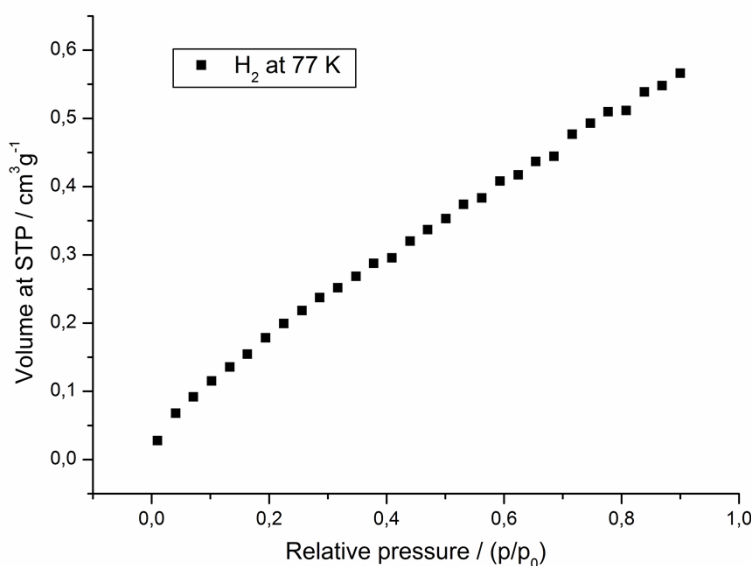


Figure S9. H₂ adsorption isotherm for activated {[Mn₂(ina)₄(H₂O)₂]·2EtOH}_n (**1as**) at 77K.

Estimation of CO₂/N₂ selectivity factor

An estimation of the CO₂/N₂ selectivity factor *S*, defined as the molar ratio of the adsorption quantities (see eqn 1 below), has been made at partial pressures of 0.15 bar for CO₂ (195 K) and 0.75 bar for H₂ (77 K). The selected pressures are relevant to post-combustion CO₂ capture.

$$S = (n_{\text{CO}_2}/n_{\text{N}_2})/(p_{\text{CO}_2}/p_{\text{N}_2}) \quad (\text{eqn. 1})$$

$$S = 9.3$$

It should be noted that this selectivity factor does not represent the actual selectivity that would result from the dosing of a mixed gas since it does not take into account the competition of CO₂ and N₂ for the adsorption sites of the activated **1as**.

The calculated factor is expected to be larger if the data for N₂ adsorption, taken for calculations, were recorded at the same temperature as for CO₂ (195 K).

References in the Supporting Information

S11. A. Altomare, M. C. Burla, M. Camalli, G. L. Cascarano, C. Giacovazzo, A. Guagliardi, A. G. G. Moliterni, G. Polidori and R. Spagna, *J. Appl. Cryst.*, 1999, **32**, 115.

S12. G. M. Sheldrick, *Acta Cryst.*, 2008, **A64**, 112.